

High-Performance and Low-Power Sub-5 nm Field-Effect Transistors Based on 7-9-7-AGNR

Hang Guo¹, Xian Zhang^{2,*}, Shuai Chen³, Li Huang^{4,†}, Yan Dong⁴, and Zhi-Xin Guo^{1,‡}

¹. State Key Laboratory for Mechanical Behavior of Materials, Center for Spintronics and Quantum System, School of Materials Science and Engineering, Xi'an Jiaotong University, Xi'an, Shaanxi, 710049, China.

². Shaanxi Key Laboratory of Surface Engineering and Remanufacturing College of Mechanical and Materials Engineering Xi'an University, Xi'an 710065, China.

³. Jinan Aviation Repair Factory, No. 600, Zhangjiazhuang, Jinan, 250000, China.

⁴ State Key Laboratory of Oral & Maxillofacial Reconstruction and Regeneration; National Clinical Research Center for Oral Diseases; Shaanxi International Joint Research Center for Oral Diseases; Department of General Dentistry and Emergency, School of Stomatology, Fourth Military Medical University, Xi'an 710032, China

* zhangxian1@outlook.com

† huanglifmmu@qq.com

‡ zxguo08@xjtu.edu.cn

This PDF file includes:

SI. Table S1: Benchmark of the ballistic performance upper limit of the sub-5 nm n-type and p-type 7-9-7-AGNR MOSFETS against the ITRS requirements for HP devices in 2028 (2013 version).

SII. Table S2: Benchmark of the ballistic performance upper limit of the sub-5 nm n-type and p-type 7-9-7-AGNR MOSFETS against the ITRS requirements for LP devices in 2028 (2013 version).

SIII. Figure S1: The test of k-points along periodic direction for the transport simulation.

SIV. Figure S2: Spatially resolved LDOS for n-type 7-9-7-AGNR FET.

SV. Figure S3: I_{DS} - V_g characteristics for the p-type 7-9-7-AGNR FETs with $V_{bis} = 0.8$ V and $V_{bis} = 0.6$ V.

SI. Table S1

Table S1. Benchmark of the ballistic performance upper limit of the sub-5 nm n-type and p-type 7-9-7-AGNR MOSFETs against the ITRS requirements for HP devices in 2028 (2013 version). The doping density is $1 \times 10^{13} \text{ cm}^{-2}$, unless otherwise specified.

	Lg(nm)	UL(nm)	SS(mV/dec)	$I_{ON}(\mu\text{A}/\mu\text{m})$	I_{ON}/I_{OFF}	$C_g(\text{fF}/\mu\text{m})$	$\tau(\text{ps})$	PDP($\text{fJ}/\mu\text{m}$)
n-type	5	4	78.954	1643.1	1.64×10^4	0.31525	0.0184	0.0182
		3	72.957	1643.0	1.64×10^4	0.21175	0.0123	0.0122
		2	68.255	1488.0	1.48×10^4	0.16235	0.0105	0.0094
		1	65.723	1987.9	1.98×10^4	0.14465	0.0069	0.0083
		0	74.204	1899.1	1.89×10^4	0.14330	0.0072	0.0083
	3	4	90.638	1643.1	1.64×10^4	0.20090	0.0117	0.0115
		3	90.434	1643.1	1.64×10^4	0.15857	0.0092	0.0091
		2	81.631	2096.9	2.09×10^4	0.14465	0.0066	0.0083
		1	76.428	2195.1	2.19×10^4	0.13800	0.0060	0.0079
		0	91.209	2195.1	2.19×10^4	0.14475	0.0063	0.0083
p-type	5	4	54.656	269.7	2.69×10^3	0.12795	0.0455	0.0074
		3	54.811	971.5	9.71×10^3	0.18750	0.0185	0.0108
		2	57.776	940.1	9.40×10^3	0.21745	0.0222	0.0125
		1	58.616	496.9	4.96×10^3	0.24785	0.0478	0.0143
		0	69.199	496.4	4.96×10^3	0.25210	0.0487	0.0145
	3	4	64.734	734.3	7.34×10^3	0.16730	0.0218	0.0096
		3	68.753	734.3	7.34×10^3	0.20900	0.0273	0.0120
		2	70.229	734.3	7.34×10^3	0.23600	0.0308	0.0136
		1	74.615	734.3	7.34×10^3	0.22935	0.0299	0.0132
		0	87.257	734.3	7.34×10^3	0.22720	0.0297	0.0131
ITRS HP	5.1	4	74.994	423.5	4.23×10^3	0.17115	0.0387	0.0098
		3	79.903	3709.8	3.70×10^4	0.17625	0.0045	0.0102
		2	81.681	4277.9	4.27×10^4	0.17645	0.0039	0.0102
		1	86.604	710.0	7.10×10^3	0.20381	0.0275	0.0117
		0	98.339	539.9	5.39×10^3	0.18352	0.0326	0.0106

SII. Table S2

Table S2. Benchmark of the ballistic performance upper limit of the sub-5 nm n-type and p-type 7-9-7-AGNR MOSFETs against the ITRS requirements for LP devices in 2028 (2013 version). The doping density is $1 \times 10^{13} \text{ cm}^{-2}$, unless otherwise specified.

	Lg(nm)	UL(nm)	SS(mV/dec)	$I_{ON}(\mu\text{A}/\mu\text{m})$	I_{ON}/I_{OFF}	$C_g(\text{fF}/\mu\text{m})$	$\tau(\text{ps})$	PDP($\text{fJ}/\mu\text{m}$)
n-type	5	4	78.954	86.0	1.72×10^6	0.31525	0.3519	0.0182
		3	72.957	920.5	1.84×10^7	0.21175	0.0220	0.0122
		2	68.255	1987.9	3.94×10^7	0.16235	0.0078	0.0094
		1	65.723	1987.9	3.94×10^7	0.14465	0.0069	0.0083
		0	74.204	1357.9	2.71×10^7	0.14330	0.0101	0.0083
	3	4	90.638			0.20090		
		3	90.434	27.0	5.4×10^5	0.15857	0.5640	0.0091
		2	81.631	226.4	4.52×10^6	0.14465	0.0610	0.0083
		1	76.428	114.9	2.28×10^6	0.13800	0.1150	0.0079
		0	91.209	5.2	1.04×10^5	0.14475		0.0083
p-type	5	4	54.656	226.0	4.52×10^6	0.12795	0.0543	0.0074
		3	54.811	920.0	1.84×10^7	0.18750	0.0195	0.0108
		2	57.776	920.0	1.84×10^7	0.21745	0.0226	0.0125
		1	58.616	596.0	1.19×10^7	0.24785	0.0399	0.0143
		0	69.199	596.0	1.19×10^7	0.25210	0.0406	0.0145
	3	4	64.734	721.0	1.44×10^7	0.16730	0.0223	0.0096
		3	68.753	721.0	1.44×10^7	0.20900	0.0278	0.0120
		2	70.229	721.3	1.44×10^7	0.23600	0.0314	0.0136
		1	74.615	689.0	1.37×10^7	0.22935	0.0319	0.0132
		0	87.257	99.4	1.98×10^6	0.22720	0.2190	0.0131
ITRS LP	5.1	4	74.994	316.6	6.32×10^6	0.17115	0.0518	0.0098
		3	79.903	515.8	1.03×10^7	0.17625	0.0328	0.0102
		2	81.681	273.9	5.46×10^6	0.17645	0.0618	0.0102
		1	86.604	153.5	3.06×10^6	0.20381	0.1270	0.0117
		0	98.339	50.4	1.08×10^6	0.18352	0.3490	0.0106

SIII. Figure S1

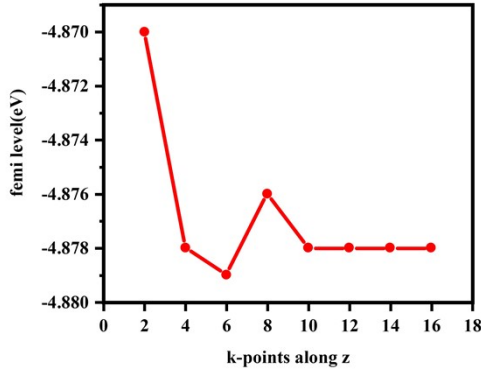


Figure S1. The test of k-points along periodic direction for the transport simulation. The simulation accuracy can be satisfactory when the number of k-point is larger than 10 along the periodic direction.

SIV. Figure S2

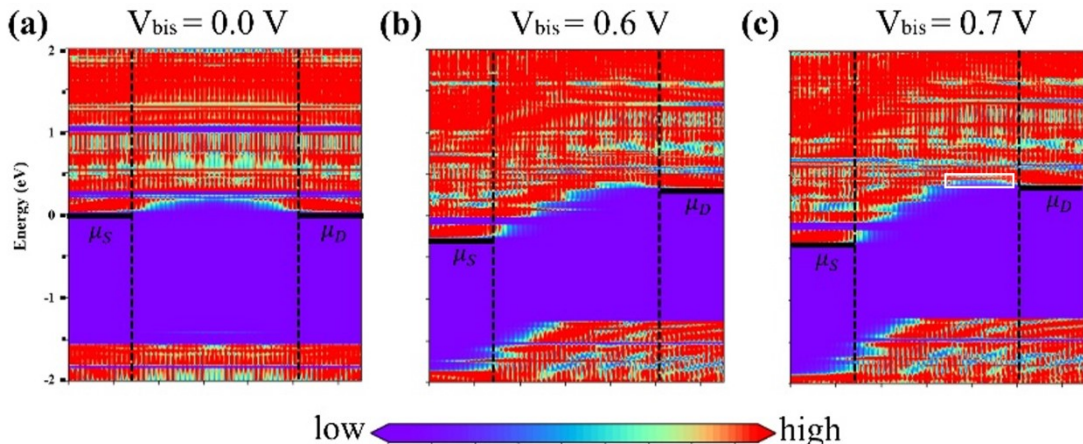


Figure S2. Spatially resolved LDOS for n-type 7-9-7-AGNR FET. (a), (b), (c) represent the LDOS of doping concentration of 1×10^{13} with $V_{\text{bis}} = 0.0, 0.6, \text{ and } 0.7 \text{ V}$, respectively. μ_S and μ_D are the electrochemical potentials of the source and drain, respectively. The white rectangle in (c) indicates the sizable energy barrier appears between the right lead and the channel region.

SV. Figure S3

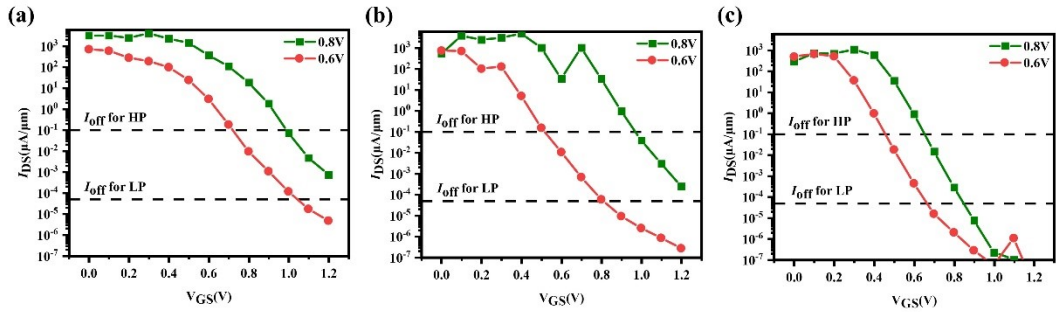


Figure R3. I_{DS} - V_g characteristics for the p-type 7-9-7-AGNR FETs with $V_{bis} = 0.8$ V (green line), $V_{bis} = 0.6$ V (red line). (a-c) are the p-type FETs with different gate lengths (1nm, 3nm, 5nm) . Note that the overlapping (L_{UL}) is set to be zero.